This manuscript is published online in Géotechnique on April 2022
DOI: https://doi.org/10.1680/jgeot.21.00245

On the isotache viscous modelling of clay behaviour using the hyperplasticity approach

Davood Dadras-Ajirloo*

Corresponding author, davood.dadrasajirlou@ntnu.no

https://orcid.org/0000-0002-8245-8124

Gustav Grimstad*

gustav.grimstad@ntnu.no

https://orcid.org/0000-0003-4433-2659

Seyed Ali Ghoreishian Amiri*

seyed.amiri@ntnu.no

https://orcid.org/0000-0003-3765-246X

* PoreLab – Centre of Excellence (SFF), Department of Civil and Environmental Engineering, Norwegian University of Science and Technology (NTNU), Trondheim, Norway

ABSTRACT

The thermodynamically based hyperplasticity framework is employed to develop a hyper-viscoplastic constitutive model describing clay's creep and rate-dependent behaviour. The proposed model complies with the concept of the isotache viscosity and the paradigm of the critical state soil mechanics that is the uniqueness of the critical state friction envelope. A versatile force potential or dissipation rate function is presented that provides adjustability of the location of the critical state while securing a unique critical state friction envelope. A non-associated flow rule as an essential property of frictional material is adopted by further development of the force potential. Adequacy of the proposed constitutive model is evaluated through the simulation of the triaxial tests conducted on Hong Kong marine deposits (HKMD).

KEYWORDS

Clays; Constitutive relations; Creep; Critical state; Rate dependence; Thermodynamics; Time dependence

LIST OF NOTATIONS

f	Helmholtz free energy potential
G	Shear modulus
g	Dimensionless shear modulus coefficient
K	Bulk modulus
k	dimensionless bulk modulus coefficient
M	slope of critical state line in p, q plot
m	exponent in power-law relationship for stiffness
n	rate sensitivity parameter
OCR	Over consolidation ratio
p	Mean effective pressure
p_0	isotropic pre-consolidation pressure associated with the reference isotache
p_0^{ref}	Reference isotropic pressure at zero plastic volumetric strain
p_a	Reference pressure (atmospheric pressure) in Helmholtz free energy potential
p_{eq}	Equivalent pressure on isotropic unloading reloading line (IURL)
q	Deviatoric stress invariant
R	Spacing ratio
r	norm of an arbitrary reference volumetric strain rate
S	State variable
T	Transition function
w	Flow potential
W^p	Plastic work
z	Force potential
v	Specific volume
ε_s^p	Deviatoric plastic strain measure
$\varepsilon_v, \varepsilon_v^p$	Total and plastic volumetric strain
γ	parameter for non-associated flow rule
η	Stress ratio invariant
κ	slope of isotropic unloading reloading line (IURL)
λ	slope of normal compression line (NCL)
μ	Creep index
τ	Intrinsic reference time, normally 24 hrs.
ν	Poisson ratio
χ_p, χ_q	Mean and deviatoric invariant of dissipative stress

INTRODUCTION

The hyperplasticity framework (Houlsby and Puzrin, 2000, Houlsby and Puzrin, 2007) provides a rigorous and systematic procedure to establish a hierarchy of thermodynamically consistent constitutive models without the unnecessary and restrictive postulate of Drucker (1957). By invoking the orthogonality postulate of Ziegler (1977), all elements of a constitutive model can be defined with the specification of two potentials: the free energy potential and dissipation rate function (or the force potential).

The hyperplastic description of the Modified Cam-Clay (MCC) model (Houlsby, 1981) has an integrable term in the increment of plastic volumetric work. This term has been considered in the free energy function by Houlsby (1981), Collins and Hilder (2002) and Collins (2005). However, Collins and Houlsby (1997) and Houlsby (2000) demonstrated that the MCC model could also be derived by putting this energy in the dissipation function. Houlsby (2018) argues that both cases can alternatively be employed to formulate families of the MCC model. Furthermore, Houlsby (2018) concluded that since there is no unique expression for the MCC model, the free energy and dissipation generally are not 'observable'.

The potential of the hyperplasticity theory has been explored rather extensively in developing rate-independent constitutive models for clay (Einav and Puzrin, 2003, Yan and Li, 2011, Coombs, 2017, Zhang et al., 2018, Rollo and Amorosi, 2020). On the contrary, its application in modelling clay's creep and rate-dependent behaviour is rare. The work by Puzrin and Houlsby (2003) is one of the pioneering attempts. They formulated a model based on 'rate process theory' (Mitchell et al., 1968, Feda, 1989) for undrained behaviour of natural clay under the triaxial condition. However, the model does not comply with the critical state soil mechanics (CSSM) in which shear and consolidation behaviour are intertwined. Later, Likitlersuang and Houlsby (2006), Likitlersuang and Houlsby (2007) and Apriadi et al. (2013), by employing the specific form of the hyperplastic MCC model with the plastic-free energy (Houlsby, 1981), proposed a rate-dependent constitutive model to capture the gradual degradation of stiffness during monotonic loading and the effect of stress history. However, the rate dependency in these models is essentially considered for simplifying the incremental formulation and the numerical integration. More recently, Jacquey and Regenauer-Lieb (2021) extended the rate-independent family of critical state models to include the rate dependency with the non-associated flow rule. However, in addition to the questionable dimension they used for viscosity, it has not been realised that the choice of using the specific form the rate-independent hyperplastic critical state model of Collins and Hilder (2002) with the plastic-free energy comes with the expensive cost of non-uniqueness of the friction mobilisation at the critical state under different loading rates.

Similarly, Aung et al. (2019) employed the hyperplasticity framework to formulate a constitutive model for soils' creep and rate-dependent behaviour. However, some serious theoretical flaws are inherent in their application of the framework, such as violation of the first law of thermodynamics and the principle of maximal rate of dissipation (Ziegler, 1977), which is the cornerstone of the hyperplasticity framework. By addressing some of these issues, Grimstad et al. (2020) proposed a hyper-viscoplastic formulation of the classical creep model (Vermeer and Neher, 1999) that was derived based on Janbu's resistance concept (Janbu, 1985).

This work is an attempt to give more clarification for the construction of hyper-viscoplastic formulation for creep and rate-dependent constitutive models that comply with the CSSM and the isotache concept. The terminology used herein follows Collins and Houlsby (1997) and Houlsby and Puzrin (2002). The force potential proposed by Grimstad et al. (2020) is derived and further developed. Particular attention is given to the model's generalisation to attain a family of isotropic isotache viscoplastic models with the non-associated flow rule while securing a unique friction envelope at the critical state. Moreover, the model is employed to simulate the behaviour of Hong Kong Marine Deposit (HKMD) (Yin and Zhu, 1999, Yin et al., 2002).

ELEMENTS AND ASSUMPTIONS

Following conventional practice, the irreversible (plastic) strain known as the internal variable and the total strain are assumed to be the kinematic variables of the system (the soil element). The formulations are strain-based. The infinitesimal strain hypothesis is adopted. The developments in the current paper are further confined to the isothermal processes for the decoupled frictional materials whose elastic moduli are independent of the internal variable. All stresses are taken to be effective stresses. Compressive stresses and strains are assumed to be positive. Two fundamental and phenomenological concepts, namely the critical state concept (Schofield and Wroth, 1968) and the isotache concept (Suklje, 1957), are invoked.

CLASSICAL FORCE AND FLOW POTENTIALS

Similar to the rate-independent case (Collins and Kelly, 2002, Collins and Hilder, 2002), the construction of the dissipation function can begin with the observation of the kinematic variables on the isotropic compression plane (Fig. 1). After Butterfield (1979), Hashiguchi (1995), and Collins and Kelly (2002), $\ln \upsilon$ (υ is specific volume) is chosen for the observation since despite other theoretical benefits it can readily resemble the volumetric strain. Therefore, according to the isotache concept (Leroueil, 2006), the rate-dependent isotropic responses of clay can be ideally depicted as Fig. 1. In order to obseve the kinematic variables and evaluate the state of the soil element, a reference state $\left(p_{ref}, \upsilon_{ref}\right)$ is defined. This is because for a system like the soil element there is no natural state to which it can return by removal of stress (Collins and Kelly, 2002).

The series of parallel lines represent the isotaches associated with normal compression lines (NCL) at different plastic strain rates. Since it is assumed that the material is decoupled and frictional, the isotropic unloading-reloading response is linear (IURL) with the slope of κ. As can be seen, in addition to the rate-independent reference state, a reference strain rate (r) (reference isotache) is also required to observe the internal variable and 'soil memory' (reserve resistance). It should be noted that the components of the reference state are independent and not work-conjugated (Collins and Kelly, 2002). The volumetric strain (ε_v), the internal variable (ε_v^p), and the soil memory (p_0) for an arbitrary state A in the compression plane are shown in Fig. 1. Following the isotache concept, rate response can be described by two equations:

$$\frac{p}{p_{ref}} = f\left(\varepsilon_v, \varepsilon_v^p\right) \tag{1}$$

$$\frac{p}{p_0} = g\left(\dot{\varepsilon}_v^p\right) \tag{2}$$

Several rheological scaling functions $\left(g\left(\dot{\varepsilon}_v^p\right)\right)$ for soft clays have been proposed (Adachi and Oka, 1982, Fodil et al., 1997, Stolle et al., 1999, Rocchi et al., 2003, Hinchberger and Rowe, 2005, Yang et al., 2016), and their applications in engineering practice have been demonstrated (Rowe and Taechakumthorn, 2008, Karstunen and Yin, 2010, Degago et al., 2011, Mirjalili et al., 2012, Karim et al., 2013, Grimstad et al., 2016, Tornborg et al., 2021). Of particular interest is the work of Stolle et al. (1999) which is consistent with Janbu's time resistance concept. This distinction provides an objective interpretation and evaluation of the time-dependent parameters (Vermeer and Neher, 1999, Grimstad et al., 2015). These parameters, as shown in Fig. 2, are the slope of the line $(n-1)$ on the bi-logarithmic plane (which is commonly used for the rheology of flows) and a reference point (p_0, r).

As can be seen, the scaling relation is logarithmically linear, whose practicality in the examination of the viscous response of several worldwide clays has been confirmed (Leroueil, 2006, Qu et al., 2010). The detailed procedure of obtaining this scaling function based on the time resistance concept is presented by Grimstad et al. (2010). The scaling relation can be expressed as:

$$\ln \frac{p}{p_{ref}} = \ln \frac{p_0}{p_{ref}} + (n-1)\left[\ln \dot{\varepsilon}_v^p - \ln r\right] \xrightarrow{yields} p = p_0 \left(\frac{\dot{\varepsilon}_v^p}{r}\right)^{(n-1)} \tag{3}$$

The rate sensitivity parameter n in equation (3), which regulates the spacing between isotaches must be larger than one. Several fundamental studies (Buisman, 1936, Suklje, 1957, Bjerrum, 1967, Garlanger, 1972) have shown that n is slightly larger than one. Indeed, according to Vermeer and Neher (1999) and Grimstad et al. (2010) n can be expressed as:

$$n = 1 + \frac{\mu}{\lambda - \kappa} \tag{4}$$

where λ and κ respectively are the slope of the NCL and IURL as shown in Fig. 1. The one-dimensional creep or secondary compression index (μ) is the creep rate (volumetric strain) in oedometer or isotropic creep tests. In the following, for simplicity, we continue to use n instead of its detailed value. r in equation (3) is the norm of an arbitrary reference volumetric strain rate which is typically taken as the average strain rate obtained in 24-h incremental loading consolidation tests.

It should be noted that p_0 and r must be evaluated consistently. They define a reference state from which the other pairs of plastic volumetric strain rate and pre-consolidation pressure are extrapolated with the scaling function. This importance has been demonstrated by Grimstad et al. (2016). According to the CSSM, p_0 can be defined as:

$$p_0 = p_{ref} \exp\left(\frac{\varepsilon_v^p}{\lambda - \kappa}\right) \tag{5}$$

in which p_{ref} is the value of p_0 at zero plastic volumetric strain. Evolution of p_0 based on equation (5), known as the isotropic hardening, renders the memory of the soil, i.e., reserve resistance against further compression.

It is of prime importance to recognize that $\dot{\varepsilon}_v^p$ as the domain of the logarithmic function (or exponentiation) in equation (3) must be strictly positive. It can become infinitesimal but never zero or negative. According to the isotache scaling function, as $\left({\dot{\varepsilon}_v^p}/{r}\right) \to 0$, then $\left({p}/{p_0}\right) \to 0$. This refers to two extreme conditions: creep and stress relaxation (a decrease of effective stress under constant volume) after an infinite time.

Based on the isotache concept, creep as a rheological phenomenon is a compressive and completely dissipative process with a progressive and one-way motion like the universal or Newtonian time, i.e., it only increases with the march of the universal time. The strict positivity of $\dot{\varepsilon}_v^p$ in equation (3) is consistent with this unidirectional attribute of creep. In other words, the bi-logarithmic compression plane (Fig. 1) comprises infinite isotaches spread to the states with unlimited logarithmic volumetric strain associated with $\dot{\varepsilon}_v^p \to 0$ at infinite time. This importance can be appreciated through the time resistance concept of Janbu (1969), which is based on the causality relation between the universal time (cause) and the creep (effect). Time here is referred to as a universal property to be differentiated from the intrinsic time defined as an inherent property of the material in the endochronic theory (Valanis, 1971). Considering the design life of infrastructures, the unlimited creep with decreasing rate has limited practical implications. For instance, in this regard, by using the isotache concept, den Haan and van den Berg (2001) reasoned that the corresponding age of clay with an over consolidation ratio (*OCR* = p/p_0) of 4 is greater than the postulated age of the universe.

Similarly, effective mean stress can theoretically relax to an infinitesimal value after an infinite time $\left(\dot{\varepsilon}_v^p \to 0\right)$. This is due to the feature of the logarithmic scaling function (equation (3)), which fits with the feature of the bi-logarithmic compression plane. The process depends on the particular choice of free energy function as it defines the state of the material. If the free energy function requires infinite volumetric elastic expansion to reach zero effective stress level (as implied by IURLs with the slope of κ), the time will clearly be limitless. Therefore, this has little practical implication again, considering the same argument as above. A detailed discussion about the performance of equation (3) in the description of the creep behaviour of clay is provided by Leoni et al. (2008) and den Haan and van den Berg (2001).

The unidirectionality attribute of isotache framework led Yin and Tong (2011), Feng et al. (2017) and Yao and Fang (2020) to consider swelling and creep as two mutually exclusive phenomena. In this regard, Alonso and Navarro (2005) provided a microstructural interpretation for the existence of distinct creep and swelling zones. On the other hand, through analyses of several experimental observations, Vergote et al. (2021) concluded that swelling is a non-isotache and essentially a transient process that strongly depends on the amount of unloading. In the light of the above, the pure plastic swelling (unlike dilation) is excluded from the current basic version of the model.

Suppose the initial state of the soil element is located at point $\mathrm{A}\left(\upsilon_A, p_{eq,A}\right)$ in Fig. 3. Now imagine the soil element undergoes an isotropic loading Δp and experience the process illustrated with the dashed grey curve in the figure. During the process, the state of the soil element shown by black dots changes and passes through different isotaches. The isotache scaling at each state is applied over the IURL associated with the related internal variable. As can be seen, the IURLs are parallel due to the assumption of the uncoupled relation between the elastic bulk modulus and the plastic strain. As a result of the history from state A to state B and the evolution of the plastic strain, the soil attains a new memory, and subsequently, the reference pre-consolidation pressure (p_0) took the relative position to the arbitrary state B ($p_{0,B}$) on the related IURL as depicted in Fig. 3. By applying the isotache scaling (equation (3)), the plastic work at the arbitrary state $\mathrm{B}(\upsilon_B, p_B)$ along the isotropic process becomes:

$$\dot{W}^p = \dot{\varepsilon}_v^p p_B = \dot{\varepsilon}_v^p p_{0,B} g(\dot{\varepsilon}_v^p) = r p_0 \left(\frac{\dot{\varepsilon}_v^p}{r}\right)^n \tag{6}$$

To exclude the plastic swelling and make the base of the exponentiation positive based on the previous discussion, equation (6) is hence modified to:

$$\dot{W}^p = r p_0 \left(\frac{\left|\dot{\varepsilon}_v^p\right| + \dot{\varepsilon}_v^p}{2r}\right)^n \tag{7}$$

Following Roscoe and Burland (1968), the shear and consolidation behaviour can be coupled via the Euclidean norm of the plastic volumetric strain and the plastic shear strain weighted by the frictional material parameter (M). The plastic work can then be expressed as:

$$\dot{W}^p = r p_0 \left(\frac{\sqrt{\left(\dot{\varepsilon}_v^p\right)^2 + \left(M \dot{\varepsilon}_s^p\right)^2} + \dot{\varepsilon}_v^p}{2r}\right)^n \tag{8}$$

Interestingly, if $n = 1$ then the dissipation function for the MCC model with the integrable term (Houlsby, 2000) can be retrieved. However, in contrast to the rate-independent case (Collins and Hilder, 2002), the plastic work rate here is completely path-dependent without any recoverable part. Therefore, herein equation (8) is considered as the dissipation rate. This is also consistent with the meaning taken for the creep in the isotache framework i.e., creep is a progressively compressive (in absence of dilatancy) and dissipative process.

Following Houlsby and Puzrin (2002), since the dissipation function in equation (8) is a homogenous function of order n, the force potential (z) can be defined as the dissipation function (equation (8)) divided by the homogeneity order n:

$$z = \frac{rp_0}{n}\left(\frac{\sqrt{\left(\dot{\varepsilon}_v^p\right)^2 + \left(M\dot{\varepsilon}_s^p\right)^2} + \dot{\varepsilon}_v^p}{2r}\right)^n \tag{9}$$

Trivially, as is the case here, the dimension of the rate of the dissipation function or force potential must be energy per volume per time equal to *stress*/*time*. However, this simple but essential point has been overlooked in some works, e.g. Aung et al. (2019) and Osman et al. (2020). Similarly, for securing a correct dimension for the dissipation function, Jacquey and Regenauer-Lieb (2021) ended up in a questionable dimension for viscosity.

The Legendre-Fenchel transformation of the force potential provides the flow potential (Houlsby and Puzrin, 2002), which defines the evolution of the internal variable (plastic strain). Following Grimstad et al. (2020), the flow potential (w) can be found:

$$w = rp_0\left(\frac{n-1}{n}\right)\left(\frac{p_{eq}}{p_0}\right)^{n/(n-1)} \tag{10}$$

where p_{eq} is known as the size of the dynamic yield surface (Perzyna, 1963), whose division by p_0 here represents the relative rate of the ongoing process. It is defined as:

$$p_{eq} = \chi_p + \frac{1}{\chi_p}\left(\frac{\chi_q}{M}\right)^2 \tag{11}$$

Equation (11) is similar to the MCC yield surface employed in the classical creep model (Vermeer and Neher, 1999), but here it is in terms of the dissipative stresses $\left(\chi_p, \chi_q\right)$. This is of prime importance since it opens a possibility to introduce a non-associated flow rule, while still obeying the principle of maximal dissipation guaranteed by Ziegler's orthogonality postulate (Ziegler, 1977, Houlsby and Puzrin, 2007). For instance, Grimstad et al. (2021) has practised this possibility to propose a relation for the evolution of the earth pressure coefficient at rest (K_0) with time.

The force potential was one of the two required potentials for constitutive modelling using the hyperplasticity approach. The free energy potential is also necessary to describe the path-independent behaviour of soil. This potential will be expressed in terms of the Helmholtz free energy in the following.

HELMHOLTZ FREE ENERGY POTENTIAL

Experimental studies on clay (Janbu, 1963, Hardin and Black, 1968, Viggiani and Atkinson, 1995, Rampello et al., 1997) indicate that the elastic behaviour is non-linearly state-dependent (stress or strain). In this regard, Houlsby et al. (2005) proposed a versatile free energy potential. The Helmholtz form (f) of this potential for the strain-based description of the current model is expressed as:

$$f = \frac{p_a}{k(2-m)}\left[\left(k(1-m)\varepsilon^*\right)^{(2-m)/(1-m)}\right] \tag{12a}$$

$$\varepsilon^* = \sqrt{\left(\varepsilon_v - \varepsilon_v^p + \frac{1}{k(1-m)}\right)^2 + \frac{3g}{k(1-m)}\left(\varepsilon_s - \varepsilon_s^p\right)^2} \tag{12b}$$

where p_a is an arbitrary reference pressure (preferably $p_a = 100$ kPa), and m, k, and g are dimensionless material parameters.

Interestingly, like the MCC dissipation function, the volumetric and shear strains in equation (12b) are coupled by the square root function. In addition to being strictly convex, the free energy potential is positive definite for any strain values, i.e., work must be done on the soil (positive work) to deform.

For an isotropic process, the bulk and shear moduli can be obtained from the free energy function as:

$$K = kp_a\left(\frac{p}{p_a}\right)^m \tag{13a}$$

$$G = gp_a \left(\frac{p}{p_a}\right)^m \tag{13b}$$

m as an exponent ($0 \leq m \leq 1$) defines the non-linearity of the pressure dependency. For $m = 1$ the bulk modulus is a linear function of pressure, and subsequently, a linear relation for IURLs on the logarithmic compression plane (Fig. 3) can be retrieved. In this case, the slope of IURLs (κ) equals $^1/_k$. This is also conforming to the CSSM definition of the soil memory (equation (5)), which in the isotache concept controls the time resistance of soil (Grimstad et al., 2010). This distinction provides an objective measurement for the viscous properties (the slope of the line in Fig. 2) from the time resistance concept, as the measures will be independent of the choice of the reference state.

For $m = 1$ the free energy function in equation (12) becomes singular. Houlsby et al. (2005) presented the Helmholtz free energy for this case as:

$$f = \left(\frac{p_a}{k}\right) \exp\left(k\left(\varepsilon_v - \varepsilon_v^p\right) + \frac{3}{2} kg\left(\varepsilon_s - \varepsilon_s^p\right)^2\right) \tag{14}$$

The volumetric and shear strains in equation (14) are still coupled to give a pressure-dependent elastic shear modulus. The byproduct of having this experimentally supported feature for the elastic stiffness is another feature called ‘stress-induced anisotropy’. This kind of anisotropy is an imposed condition on the system by the first law of thermodynamic and is not related to the fundamental structure of the material. In this case, according to Muir Wood and Graham (1990), for a non-isotropic process, the unloading-reloading behaviour on the compression plane is not a single line but rather an unloading- reloading region whose size and shape depend on the stress field. This is shown schematically in Fig. 4.

Perhaps the most striking feature of the free energy potential is lack of the plastic-free energy or stored plastic work. For the rate-independent case, Collins and Hilder (2002) have proposed a family of the CSSM model by modifying the flow rule and the location of the critical state via adjustment of shares of the stored and the dissipated plastic work. Based on Ziegler's orthogonality postulate, the plastic-free energy gives a rate-independent 'shift' or 'back' stress that relates the true stress to the dissipative stress (Collins and Houlsby, 1997). Grimstad et al. (2020) demonstrated that plastic-free energy could not be included for a rate-dependent system with a single internal variable. Otherwise, there would be no unique mobilised friction at the critical state, which contradicts the paradigm of CSSM (Schofield and Wroth, 1968). This is because the plastic-free energy must be a unique function of the internal variable, not its rate. Whereas the creep or the rate-dependency of the material behaviour is essentially a history or path-dependent (loading history), i.e., they must be considered in the dissipation function of the rate of the internal variable.

On the other hand, based on the interpretation of Collins (2005), ignoring the stored plastic work imposes a homogenous volumetric mechanism at the micro/mesoscale. Therefore, by acknowledging this limitation that dissipative and true stress are equal (no shift stress), the following focuses on devising a sophisticated force potential to attain a versatile flow rule and an adjustable critical state location on the unique critical state friction envelope.

GENERALISATION OF THE FORCE AND FLOW POTENTIALS

The force potential defined in equation (9) provides the classical viscoplastic model (Vermeer and Neher, 1999). The model's performance in the true stress space is schematically shown in Fig. 5. As can be seen, there are three MCC elliptical surfaces with homothetic relations. Each p_{eq} is a function of an elliptical convex set of the deviatoric and the mean stresses. The homothetic relation between the convex sets or the ratio of ${}^{p_{eq}}/_{p_0}$ determines the relative rate of the loading of a certain process. As a result, the critical state is always located in the middle of the ellipses. In other words, the ratio of the equivalent stress measure to the isotropic component of the corresponding critical state stress, known as 'Spacing Ratio', is always equal to two. However, experimental studies show that this is not the general case, and higher values for spacing ratio have been reported for clay (Chakraborty et al., 2013, Chen and Yang, 2017).

To redress this limitation, the force potential in equation (9) is modified to:

$$z = \frac{rp_0}{n}\left(\frac{\sqrt{\left(T\dot{\varepsilon}_v^p\right)^2 + \left(M\dot{\varepsilon}_s^p\right)^2} + \dot{\varepsilon}_v^p}{Rr}\right)^n \tag{15}$$

where R >1 is the spacing ratio. Every other parameter in equation (15) is the same as equation (9) except the first term inside the square root, which is called the transition function:

$$T = \frac{R}{2} + \left(\frac{R-2}{2}\right)\tanh(S) \tag{16}$$

where S is a state variable defined as:

$$S = \left(\frac{M}{\eta}\right)^2 - \left(\frac{\eta}{M}\right)^2 \tag{17a}$$

$$\eta = {}^{q}/_{p} \tag{17b}$$

Considering the homothetic functioning of isotache framework, the critical state stress ratio is taken as a reference in the definition of the state variable. The stress ratio η can represent the mobilised friction at the current stress state. For $R = 2$, the transition function will be independent of η, and the force potential in equation (9) can be retrieved. Again following Houlsby and Puzrin (2002) and Grimstad et al. (2020), the same structure for the flow potential as equation (10) can be obtained in which p_{eq} is expressed in terms of dissipative stress as:

$$p_{eq} = \frac{R\chi_p\sqrt{\left(\chi_p^2M^2 - \chi_q^2\right)^2 + \chi_q^2\left(MT\chi_p + \sqrt{\chi_p^2M^2 + (T^2-1)\chi_q^2}\right)^2}}{T\left(\chi_p^2M^2 - \chi_q^2\right) + \sqrt{\left(\chi_p^2M^2 - \chi_q^2\right)^2 + \chi_q^2\left(MT\chi_p + \sqrt{\chi_p^2M^2 + (T^2-1)\chi_q^2}\right)^2}} \tag{18}$$

Since there is no shift stress, $\chi_p = p$ and $\chi_q = q$. In Fig. 6, the convex sets (solid curves) for $R = 1.5, 3$ in the normalised true stress space are illustrated. The other two elliptical surfaces shown by the circle and square marks are just drawn to explain the performance of the transition function T. As it is seen, the centre of the ellipses is located at the desired spacing ratio R. This is ensured by fixing the share of the plastic volumetric strain outside of the square root in the force potential to be $1/_R$. Considering the property of the hyperbolic tangent function in T, when $\eta = 0$ and subsequently $S = +\infty$, then $T = R - 1$. In this case, the force potential resembles equation (6) for any values of R describing the dissipative isotropic compression process. However, by increasing η^2 on the compressive side of the critical state stress ratio, the stress state moves along the ellipse with square marks whose size depends on the share of the plastic volumetric strain inside the square root through T. As η approaches M, the stress state slightly diverges from the ellipse with square marks towards the one with circle marks which has a different size due to change of T with η^2.

On the other hand, on the dilative side of the critical state stress ratio, with the decrease of η^2 from $+\infty$ at the extreme state $p = 0$ towards M^2at the critical state, the stress state moves along the ellipse shown by circle marks. One should bear in mind that $p = 0$ is an unapproachable state because of the chosen free energy (equation (14)) and the isotache scaling functions. Like the compressive side, as η approaches M, the stress state slightly diverges from the ellipse shown by circle marks to the one with square marks through changes in T. The fact that dilation is controlled by the ratio of the current stress ratio (η) to the critical state stress ratio and the spacing ratio (R) is a fundamental premise of the CSSM for isotropic soils, which has been employed in the current model via the versatile force potential (equation (15)). Fig. 7 shows the convex sets and related inelastic flow directions in the normalised true stress space for different values of the spacing ratio. As shown, the inelastic flow directions are practically associated, although the force potential in equation (15) involves the true stress terms in the transition function.

With an adjustable spacing ratio, the model can now compete with the analogue viscoplastic models (Kutter and Sathialingam, 1992, Yin and Zhu, 1999, Yin et al., 2002, Islam and Gnanendran, 2017). These models pursue associated flow rule as they are based on the viscoplastic theory of Perzyna (1963) proposed by invoking the postulate of Drucker (1957). Moreover, these models use a composite dynamic surface presented by Dafalias and Herrmann (1986), which can cause their numerical integration problematic. In contrast, the proposed model up to this stage can continuously describe a process with the single and convex sets of dissipative stresses defined in equation (18). This distinction allows the employment of particular numerical schemes (de Borst and Heeres, 2002, Simo and Hughes, 2006) to integrate the proposed constitutive model. Despite this distinction, the proposed model still practically suffers from the associated flow rule. According to Collins and Kelly (2002), this deficiency stems from a lack of the essential property of frictional material that is the pressure-dependent frictional dissipative mechanism. This deficiency can be overcome by introducing a linear frictional dissipation mechanism to the force potential (equation (15)) via rewriting M as a linear function of the true mean stress p. Therefore, by preserving the dimension of the force potential and considering the boundaries, namely the critical state shearing and isotropic compression, as two mutually exclusive processes, M in equations (15) and (18) can be replaced by $\overline{M}$ defined as:

$$\overline{M} = M\left[1 - \gamma + \gamma\left(\frac{Rp}{\bar{p}_0}\right)\right] \tag{19a}$$

$$\bar{p}_0 = \frac{Rp\sqrt{(p^2M^2 - q^2)^2 + q^2\left(MTp + \sqrt{p^2M^2 + (T^2 - 1)q^2}\right)^2}}{T(p^2M^2 - q^2) + \sqrt{(p^2M^2 - q^2)^2 + q^2\left(MTp + \sqrt{p^2M^2 + (T^2 - 1)q^2}\right)^2}} \tag{19b}$$

where γ is a positive value parameter interpolating M between mutually exclusive states of $\eta = 0$, $\eta = M$ and $\eta = \pm\infty$. To increase the flexibility in fine-tuning the value of γ, it is suggested to employ the following equation instead of equation (19a):

$$\overline{M} = M\sqrt{1-\gamma+\gamma\left(\frac{Rp}{\bar{p}_0}\right)} \qquad (20)$$

Fig. 8 depicts the new convex loci together with the inelastic flow directions in the normalised true stress plane for different values γ. As can be seen, the frictional dissipative mechanism, which is intensified by the increase of γ value, pushes the loci towards more "tear-drop" shapes. However, the loci remain convex as it must, even for relatively high values of γ. Unlike the rate-independent case (Collins and Kelly, 2002), convexity in the true stress space, as well as the dissipative stress space, is necessary for isotache viscoplastic models. Otherwise, the concave parts of loci would shrink as the loading rate increases causing lower shear strength for high loading rates, which contradicts the experimental observations.

As another substantial distinction shown in Fig. 8, it can be observed that whilst the critical state location remains unchanged, the intensification of the frictional mechanism mitigates the dilatancy on the dilative side of the critical state envelope, whereas it relatively increases the dilatancy on the compressive side of the critical state envelope.

MODEL PARAMETERS

Equations (13), (10), (9) and (18) define all components of the proposed model. These equations can be compacted into two potentials since the combination of the last three equations is the flow potential (equation (10)). Based on these equations, the current model requires seven dimensionless parameters. These parameters can straightforwardly be evaluated from conventional triaxial and oedometer tests. Table 1 shows the model parameters and their value for HKMD.

Three parameters κ, λ and M are the traditional parameters of the CSSM. k and g specify the elastic moduli. As it has been assumed $m = 1$ in equation (13), the slope of IURL (κ) is equal to $1/_k$. Based on the free energy function (equation (14)), there is no stress-induced anisotropy for isotropic loading processes (Houlsby et al., 2005). Subsequently, a constant Poisson's ratio (ν) for isotropic stress condition can be retrieved:

$$\frac{G}{K} = \frac{g}{k} = \frac{3(1-2\nu)}{2(1+\nu)} \approx 0.75 \tag{21}$$

In the absence of the proper experimental data for small strain conditions, equation (21) can be employed for the estimation of g.

Parameters R and γ adjust the shape of the convex locus. The locus equivalently represents the yield surface for the rate-independent condition. Specifically, spacing ratio R determines the relative location of the critical state on the convex set or the location of the critical state line from the NCL on the compression plane. By reviewing the experimental observation, Chen and Yang (2017) demonstrated that R varies typically between two and three for clay. A positive value for parameter γ specifies the degree of non-associativity in the flow rule. As it increases, the convex surface becomes more twisted and shows significant stress softening on the compressional side of the critical state line. For $\gamma = 0$ the flow rule is practically associated, as shown in Fig. 7 and 8.

The creep index (μ) is the rate of creep in the oedometer or isotropic creep tests. Based on this definition, it is tempting to estimate the value of μ by plotting the creep data in terms of strain against the logarithm of time. However, this would result in an unobjective value for μ depending on subjective appreciation of the curvature of the plotted response. This is of great importance since a slight change in the value of μ significantly affect the creep or rate-dependent response of the model. For an objective value of μ, according to the time resistance concept (Janbu, 1969, Janbu, 1985), the creep data should be plotted in the form of the inverse of strain rate (time resistance) against time which results in a linear pattern whose slope is equal to ${}^{1}/_{\mu}$ (Vermeer and Neher, 1999, Grimstad et al., 2015). Alternatively, according to Nash and

Ryde (2001), μ can also be objectively determined by plotting the creep data in terms of strain against the logarithm of strain rate and computing the slope of the trendline.

The arbitrary reference strain rate (r) is usually taken to be the norm of the average volumetric strain rate obtained in 24-h incremental loading consolidation tests such as oedometer (K_0 loading) or isotropic consolidation. For instance, for the oedometer test, the plastic strain rate under K_0 loading can be written as:

$$\dot{\varepsilon}_v^p\Big|_{oed} = \frac{\partial w}{\partial \chi_p} = r\left(\frac{p_{eq}}{p_0}\right)^{\frac{\mu}{\lambda-\kappa}} \frac{\partial p_{eq}}{\partial \chi_p}\bigg|_{\eta_{k0}} \tag{22}$$

in which, equation (4) is employed for n. Since the isotache associated with the K_0-loading $(\eta = \eta_{K0})$ is chosen as the reference, $p_{eq} = p_0$ and therefore r can be computed as:

$$r = \frac{\dot{\varepsilon}_v^p\Big|_{oed}}{\frac{\partial p_{eq}}{\partial \chi_p}\bigg|_{\eta_{K0}}} = \frac{\mu}{\tau\left(\frac{\partial p_{eq}}{\partial \chi_p}\bigg|_{\eta_{K0}}\right)} \tag{23}$$

in which, $\dot{\varepsilon}_v^p\big|_{oed}$ is replaced by its value ${}^{\mu}/_{\tau}$ according to the time resistance concept (Grimstad et al., 2010). Note that since there is no shift stress, $\chi_p = p$ should be employed in equation (22) and (23). τ is the intrinsic reference time which is normally taken to be 24-h for an odometer test.

EVALUATION OF MODEL

To evaluate the adequacy of the proposed model, triaxial tests conducted by Zhu (2000) on the reconstituted samples of the HKMD are simulated. The model parameters presented in Table 1 are obtained based on the data reported by Yin and Zhu (1999), Zhu (2000), and Yin et al. (2002).

Fig. 9 shows the simulated and measured data of undrained triaxial compression tests at constant strain loading rates of 0.15, 1.5, and 15%/h. Before shearing, each specimen was normally consolidated to isotropic mean effective stress of 400 kPa ($p_0 = 400\ kPa$). Except for the case of $R = 2$ (the MCC dynamic surface) at the strain rate of 15%/h, there is a reasonable agreement between the simulations and the experiments. The simulation with $R = 2$ demonstrates the significant effect of the spacing ratio parameter on the predicted undrained shear strength. In fact, the ratio of the shear strength when $R = 2$ to the one when $R = 2.5$ is equal to the inverse of the ratio of their correspondent spacing ratios.

Fig. 10 shows the comparison between the measurements and the simulations of undrained triaxial tests at the strain rate of 1.5%/h conducted on the specimens with different over-consolidation ratios (*OCR*). The model captures the response of the lightly overconsolidated samples (*OCR* = 1, 2) well. However, the responses of the specimens with *OCR* of 4 and 8 are overestimated. This is even worse for the case of *OCR* = 8 using the MCC dynamic surface. The measurements depict a hardening behaviour all over the test. However, the model exhibits softening response after attaining the peak stress at axial strains between 1% and 2%. This is the identical drawback seen in the MCC model that can be overcome by considering the stiffness degradation through the introduction of kinematic hardening (Houlsby, 2000, Einav and Puzrin, 2003).

The undrained triaxial test with complicated loading stages shown in Table 2 is also simulated. An initial effective cell pressure of 300 kPa is considered for the normally consolidated sample. The comparison between the simulation and the measurements can be seen in Fig. 11. The Simulations have also been done with the constant shear modulus (*G*) of 9200 kPa to assess the effect of the stress-induced anisotropy imposed by the first law of thermodynamic. According to Fig. 11(a), the stress-strain response of both simulations is quite similar with an acceptable agreement with the measurements. However, Fig. 11(b) shows some differences between the simulations of developed excess pore water pressure. The result of both simulations are generally in agreement with the measurements, but the simulation with constant *G* shows more sensitivity in the excess pore water pressure to the change of loading rate, particularly for relaxations and the subsequent reloading parts. The difference between the two simulations can be observed clearly in the stress path shown in Fig. 11(c). Due to the stress-induced anisotropy, the stress path for the case with pressure-dependent shear modulus is inclined and indicates better agreement with the measurements in the early stages of the test. However, in both cases, the model could not satisfactorily capture the reloading after the unloading stage and consequently the relaxations and the subsequent reloading stages.

CONCLUSIONS

This paper demonstrates the application of the hyperplasticity approach in the development of a constitutive model to characterise the creep and rate-dependent behaviour of clays. The compliance with the concepts of critical state and the isotache viscosity is considered. The proposed model is specified by defining the free energy and force potentials. The force potential for the classical creep model is derived and further developed for a wide range of clays by considering the spacing ratio. The developed model enjoys the non-associated flow rule as a natural consequence of the frictional dissipative mechanism. It requires seven dimensionless material parameters. Some of the model's distinctive features, namely adjustability of the critical state location and stress-induced anisotropy, are validated by simulation of the triaxial tests conducted on the reconstituted HKMD clay.

Compliance with the uniqueness of the critical state friction envelope rejects the plastic part of the free energy for a system with a single internal variable. A promising remedy for this deficiency could be the introduction of additional internal variables, which might help model the pure plastic swelling behaviour. Moreover, further development of the model can include the Lode angle dependency, the plastic anisotropy, and the destructuration, which are all notable features of the mechanical behaviour of clays.

ACKNOWLEDGEMENTS

The authors would like to acknowledge the support from the Research Council of Norway through its Centres of Excellence Funding Scheme, PoreLab, project number 262644. The authors appreciate the valuable discussions and support from Prof. Steinar Nordal and Prof. Gudmund Reidar Eiksund.

REFERENCES

Adachi, T. & Oka, F. (1982) Constitutive equations for normally consolidated clay based on elasto-viscoplasticity. *Soils Found.* **22(4)**:57-70.

Alonso, E. E. & Navarro, V. (2005) Microstructural model for delayed deformation of clay: loading history effects. *Canadian Geotechnical Journal* **42(2)**:381-392.

Apriadi, D., Likitlersuang, S. & Pipatpongsa, T. (2013) Loading path dependence and non-linear stiffness at small strain using rate-dependent multisurface hyperplasticity model. *Computers and Geotechnics* **49**:100-110.

Aung, Y., Khabbaz, H. & Fatahi, B. (2019) Mixed hardening hyper-viscoplasticity model for soils incorporating non-linear creep rate–H-creep model. *International Journal of Plasticity* **120**:88-114.

Bjerrum, L. (1967) Engineering geology of Norwegian normally-consolidated marine clays as related to settlements of buildings. *Géotechnique* **17(2)**:83-118.

Buisman, A. (1936) Results of long duration settlement tests. In *Proc. 1st ICSMFE*.) Cambridge, vol. 1, pp. 103-107.

Butterfield, R. (1979) A natural compression law for soils (an advance on e–log p′). *Géotechnique* **29(4)**:469-480.

Chakraborty, T., Salgado, R. & Loukidis, D. (2013) A two-surface plasticity model for clay. *Computers and Geotechnics* **49**:170-190.

Chen, Y. N. & Yang, Z. X. (2017) A family of improved yield surfaces and their application in modeling of isotropically over-consolidated clays. *Computers and Geotechnics* **90**:133-143.

Collins, I. & Houlsby, G. (1997) Application of thermomechanical principles to the modelling of geotechnical materials. *Proceedings of the Royal Society of London. Series A: Mathematical, Physical and Engineering Sciences* **453(1964)**:1975-2001.

Collins, I. F. (2005) The concept of stored plastic work or frozen elastic energy in soil mechanics. *Géotechnique* **55(5)**:373-382.

Collins, I. F. & Hilder, T. (2002) A theoretical framework for constructing elastic/plastic constitutive models of triaxial tests. *International Journal for Numerical and Analytical Methods in Geomechanics* **26(13)**:1313-1347.

Collins, I. F. & Kelly, P. A. (2002) A thermomechanical analysis of a family of soil models. *Géotechnique* **52(7)**:507-518.

Coombs, W. M. (2017) Continuously unique anisotropic critical state hyperplasticity. *International Journal for Numerical and Analytical Methods in Geomechanics* **41(4)**:578-601.

Dafalias, Y. F. & Herrmann, L. R. (1986) Bounding Surface Plasticity. II: Application to Isotropic Cohesive Soils. *Journal of Engineering Mechanics* **112(12)**:1263-1291.

De Borst, R. & Heeres, O. M. (2002) A unified approach to the implicit integration of standard, non-standard and viscous plasticity models. *International Journal for Numerical and Analytical Methods in Geomechanics* **26(11)**:1059-1070.

Degago, S. A., Grimstad, G., Jostad, H. P., Nordal, S. & Olsson, M. (2011) Use and misuse of the isotache concept with respect to creep hypotheses A and B. *Géotechnique* **61(10)**:897-908.

Den Haan, E. J. & Van Den Berg, P. (2001) *Evaluation of creep models for soft soils (under axially symmetric conditions)*. Delft, the Netherlands.

Drucker, D. C. (1957) *A definition of stable inelastic material*.

Einav, I. & Puzrin, A. M. (2003) Evaluation of continuous hyperplastic critical state (CHCS) model. *Géotechnique* **53(10)**:901-913.

Feda, J. (1989) Interpretation of creep of soils by rate process theory. *Géotechnique* **39(4)**:667-677.

Feng, W.-Q., Lalit, B., Yin, Z.-Y. & Yin, J.-H. (2017) Long-term Non-linear creep and swelling behavior of Hong Kong marine deposits in oedometer condition. *Computers and Geotechnics* **84**:1-15.

Fodil, A., Aloulou, W. & Hicher, P. Y. (1997) Viscoplastic behaviour of soft clay??? *Géotechnique* **47(3)**:581-591.

Garlanger, J. E. (1972) The consolidation of soils exhibiting creep under constant effective stress. *Géotechnique* **22(1)**:71-78.

Grimstad, G., Dadrasajirlou, D. & Amiri, S. a. G. (2020) Modelling creep in clay using the framework of hyper-viscoplasticity. *Géotechnique Letters* **10(3)**:404-408.

Grimstad, G., Degago, S. A., Nordal, S. & Karstunen, M. (2010) Modeling creep and rate effects in structured anisotropic soft clays. *Acta Geotechnica* **5(1)**:69-81.

Grimstad, G., Haji Ashrafi, M. A., Degago, S. A., Emdal, A. & Nordal, S. (2016) Discussion of 'Soil creep effects on ground lateral deformation and pore water pressure under embankments'. *Geomechanics and Geoengineering* **11(1)**:86-93.

Grimstad, G., Long, M., Dadrasajirlou, D. & Amiri, S. a. G. (2021) Investigation of Development of the Earth Pressure Coefficient at Rest in Clay During Creep in the Framework of Hyper-Viscoplasticity. *International Journal of Geomechanics* **21(1)**:04020235.

Grimstad, G., Mehli, M. & Degago, S. A. (2015) Creep in clay during the first few years after construction. In *Deformation Characteristics of Geomaterials*.) IOS Press, pp. 915-922.

Hardin, B. O. & Black, W. L. (1968) Vibration Modulus of Normally Consolidated Clay. *Journal of the Soil Mechanics and Foundations Division* **94(2)**:353-369.

Hashiguchi, K. (1995) On the linear relations of V–ln p and ln v–ln p for isotropic consolidation of soils. *International Journal for Numerical and Analytical Methods in Geomechanics* **19(5)**:367-376.

Hinchberger, S. D. & Rowe, R. K. (2005) Evaluation of the predictive ability of two elastic-viscoplastic constitutive models. *Canadian Geotechnical Journal* **42(6)**:1675-1694.

Houlsby, G. (2000) Critical state models and small-strain stiffness. In *Developments in Theoretical Geomechanics. Proceedings of the Booker Memorial Symposium*.) Citeseer, pp. 295-312.

Houlsby, G. T. (1981) Study of plasticity theories and their applicability to soils.) University of Cambridge.

Houlsby, G. T. (2018) *Hyperplasticity*, See https://hyperplasticity.files.wordpress.com/2018/11/t138_2018_h_purdue_hyperplasticity.pdf.

Houlsby, G. T., Amorosi, A. & Rojas, E. (2005) Elastic moduli of soils dependent on pressure: a hyperelastic formulation. *Géotechnique* **55(5)**:383-392.

Houlsby, G. T. & Puzrin, A. M. (2000) A thermomechanical framework for constitutive models for rate-independent dissipative materials. *International Journal of Plasticity* **16(9)**:1017-1047.

Houlsby, G. T. & Puzrin, A. M. (2002) Rate-dependent plasticity models derived from potential functions. *Journal of Rheology* **46(1)**:113-126.

Houlsby, G. T. & Puzrin, A. M. (2007) *Principles of hyperplasticity: an approach to plasticity theory based on thermodynamic principles.* Springer Science & Business Media.

Islam, M. N. & Gnanendran, C. T. (2017) Elastic-Viscoplastic Model for Clays: Development, Validation, and Application. *Journal of Engineering Mechanics* **143(10)**:04017121.

Jacquey, A. B. & Regenauer-Lieb, K. (2021) Thermomechanics for Geological, Civil Engineering and Geodynamic Applications: Rate-Dependent Critical State Line Models. *Rock Mechanics and Rock Engineering*.

Janbu, N. (1963) Soil compressibility as determined by odometer and triaxial tests. In *Proc. Europ. Conf. SMFE*.), vol. 1, pp. 19-25.

Janbu, N. (1969) The resistance concept applied to deformations of soils. In *Proceedings of the 7th International Conference on Soil Mechanics and Foundation Engineering*.), Mexico City, vol. 2529, pp. 191-196.

Janbu, N. (1985) Soil models in offshore engineering. *Géotechnique* **35(3)**:241-281.

Karim, M. R., Oka, F., Krabbenhoft, K., Leroueil, S. & Kimoto, S. (2013) Simulation of long-term consolidation behavior of soft sensitive clay using an elasto-viscoplastic constitutive model. *International Journal for Numerical and Analytical Methods in Geomechanics* **37(16)**:2801-2824.

Karstunen, M. & Yin, Z.-Y. (2010) Modelling time-dependent behaviour of Murro test embankment. *Géotechnique* **60(10)**:735-749.

Kutter, B. L. & Sathialingam, N. (1992) Elastic-viscoplastic modelling of the rate-dependent behaviour of clays. *Géotechnique* **42(3)**:427-441.

Leoni, M., Karstunen, M. & Vermeer, P. A. (2008) Anisotropic creep model for soft soils. *Géotechnique* **58(3)**:215-226.

Leroueil, S. (2006) The Isotache approach. Where are we 50 years after its development by Professor Šuklje? Prof. Šuklje's Memorial Lecture. In *Proc. 13th Danube Eur. Conf. on Geotech. Engng*.), Ljubljana, vol. 1, pp. 55-88.

Likitlersuang, S. & Houlsby, G. T. (2006) Development of hyperplasticity models for soil mechanics. *International Journal for Numerical and Analytical Methods in Geomechanics* **30(3)**:229-254.

Likitlersuang, S. & Houlsby, G. T. (2007) Predictions of a continuous hyperplasticity model for Bangkok clay. *Geomechanics and Geoengineering* **2(3)**:147-157.

Mirjalili, M., Kimoto, S., Oka, F. & Hattori, T. (2012) Long-term consolidation analysis of a large-scale embankment construction on soft clay deposits using an elasto-viscoplastic model. *SOILS AND FOUNDATIONS* **52(1)**:18-37.

Mitchell, J. K., Campanella, R. G. & Singh, A. (1968) Soil Creep As A Rate Process. *Journal of the Soil Mechanics and Foundations Division* **94(1)**:231-253.

Muir Wood, D. & Graham, J. (1990) Anisotropic elasticity and yielding of a natural plastic clay. *International Journal of Plasticity* **6(4)**:377-388.

Nash, D. F. T. & Ryde, S. J. (2001) Modelling consolidation accelerated by vertical drains in soils subject to creep. *Géotechnique* **51(3)**:257-273.

Osman, A. S., Birchall, T. J. & Rouainia, M. (2020) A simple model for tertiary creep in geomaterials. *Geotechnical Research* **7(1)**:26-39.

Perzyna, P. (1963) The constitutive equations for rate sensitive plastic materials. *Quarterly of Applied Mathematics* **20(4)**:321-332.

Puzrin, A. M. & Houlsby, G. T. (2003) Rate-Dependent Hyperplasticity with Internal Functions. *Journal of Engineering Mechanics* **129(3)**:252-263.

Qu, G., Hinchberger, S. D. & Lo, K. Y. (2010) Evaluation of the viscous behaviour of clay using generalised overstress viscoplastic theory. *Géotechnique* **60(10)**:777-789.

Rampello, S., Viggiani, G. M. B. & Amorosi, A. (1997) Small-strain stiffness of reconstituted clay compressed along constant triaxial effective stress ratio paths. *Géotechnique* **47(3)**:475-489.

Rocchi, G., Fontana, M. & Prat, M. D. (2003) Modelling of natural soft clay destruction processes using viscoplasticity theory. *Géotechnique* **53(8)**:729-745.

Rollo, F. & Amorosi, A. (2020) SANICLAY-T: simple thermodynamic-based anisotropic plasticity model for clays. *Computers and Geotechnics* **127**:103770.

Roscoe, K. & Burland, J. (1968) On the generalized stress-strain behaviour of 'wet clay'. In *Engineering plasticity*. (Heyman, J., andLeckie, F. (eds)) Cambridge University Press, Cambridge, pp. 535-609.

Rowe, R. K. & Taechakumthorn, C. (2008) Combined effect of PVDs and reinforcement on embankments over rate-sensitive soils. *Geotextiles and Geomembranes* **26(3)**:239-249.

Schofield, A. N. & Wroth, P. (1968) *Critical state soil mechanics.* McGraw-hill London.

Simo, J. C. & Hughes, T. J. (2006) *Computational inelasticity.* Springer Science & Business Media.

Stolle, D., Vermeer, P. A. & Bonnier, P. G. (1999) A consolidation model for a creeping clay. *Canadian Geotechnical Journal* **36(4)**:754-759.

Suklje, L. (1957) The analysis of the consolidation process by the isotaches method. In *Proc. 4th Int. Conf. Soil Mech. Found. Engng*.), London, vol. 1, pp. 319-326.

Tornborg, J., Karlsson, M., Kullingsjö, A. & Karstunen, M. (2021) Modelling the construction and long-term response of Göta Tunnel. *Computers and Geotechnics* **134**:104027.

Valanis, K. (1971) A theory of viscoplasticity without a yield surface. *Arch. Mech. Stos.* **23(4)**:515-553.

Vergote, T. A., Leung, C. F. & Chian, S. C. (2021) Modelling creep and swelling after unloading under constant load and relaxation with Bayesian updating. *Géotechnique* **0(0)**:1-14.

Vermeer, P. & Neher, H. (1999) A soft soil model that accounts for creep. In *Beyond 2000 in computational geotechnics*.) Routledge, pp. 249-261.

Viggiani, G. & Atkinson, J. H. (1995) Stiffness of fine-grained soil at very small strains. *Géotechnique* **45(2)**:249-265.

Yan, W. M. & Li, X. S. (2011) A model for natural soil with bonds. *Géotechnique* **61(2)**:95-106.

Yang, C., Carter, J. P., Sheng, D. & Sloan, S. W. (2016) An isotach elastoplastic constitutive model for natural soft clays. *Computers and Geotechnics* **77**:134-155.

Yao, Y.-P. & Fang, Y.-F. (2020) Negative creep of soils. *Canadian Geotechnical Journal* **57(1)**:1-16.

Yin, J.-H. & Tong, F. (2011) Constitutive modeling of time-dependent stress–strain behaviour of saturated soils exhibiting both creep and swelling. *Canadian Geotechnical Journal* **48(12)**:1870-1885.

Yin, J.-H. & Zhu, J.-G. (1999) Measured and predicted time-dependent stress-strain behaviour of Hong Kong marine deposits. *Canadian Geotechnical Journal* **36(4)**:760-766.

Yin, J.-H., Zhu, J.-G. & Graham, J. (2002) A new elastic viscoplastic model for time-dependent behaviour of normally and overconsolidated clays: theory and verification. *Canadian Geotechnical Journal* **39(1)**:157-173.

Zhang, Z., Chen, Y. & Huang, Z. (2018) A novel constitutive model for geomaterials in hyperplasticity. *Computers and Geotechnics* **98**:102-113.

Zhu, J.-G. (2000) Experimental study and elastic visco-plastic modelling of the time-dependent stress-strain behaviour of Hong Kong marine deposits. In *Dept. of Civil and Structural Engineering*.) Hong Kong Polytechnic University, Hung Hom, Hong Kong, vol. Ph.D.

Ziegler, H. (1977) *An introduction to thermodynamics.* North-Holland Publishing Company.

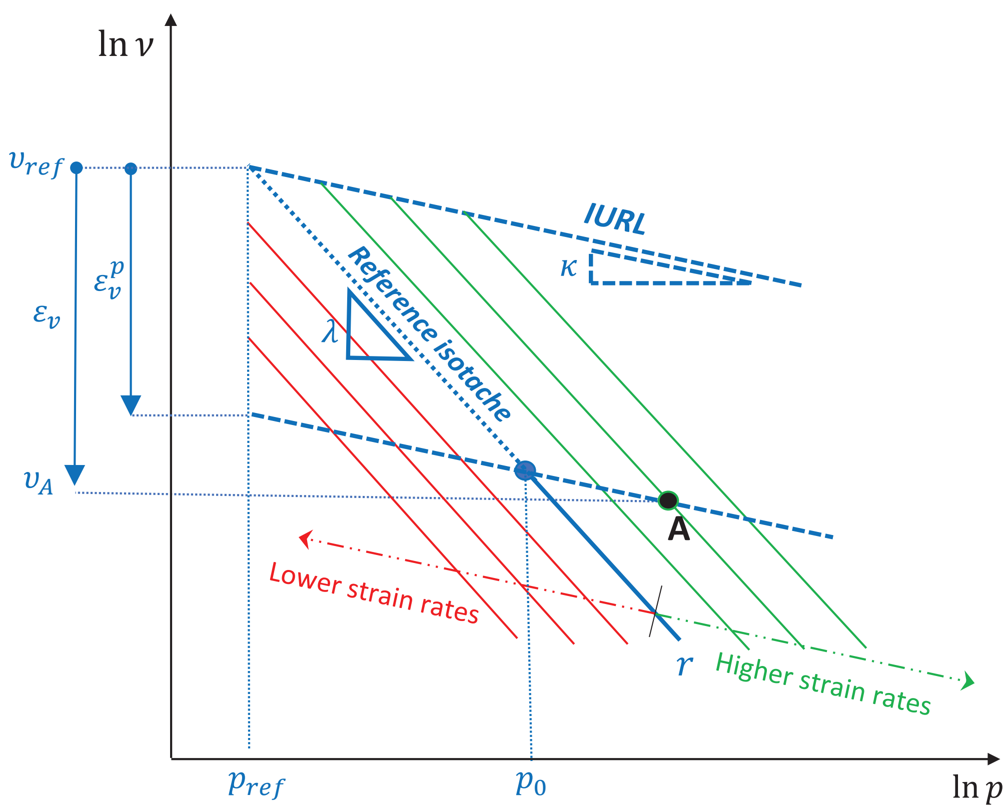

Fig. 1: Isotache idealization of rate-dependent isotropic compression behaviour of soil and illustration of the reference state

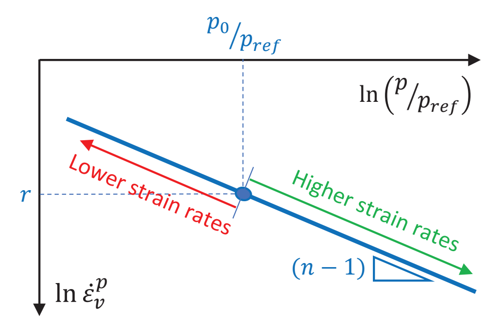

Fig. 2: Isotache scaling relation

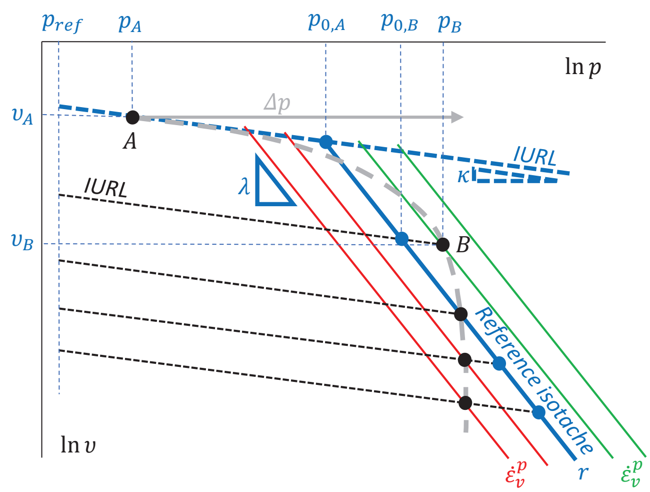

Fig. 3: Illustration of an arbitrary isotropic consolidation process and application of isotache scaling relation along the process

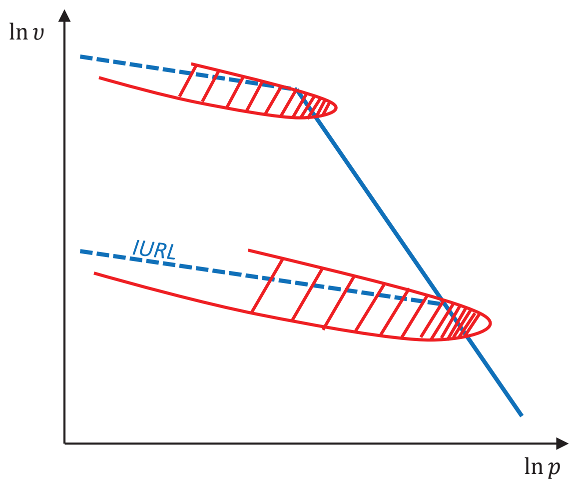

Fig. 4: Unloading- reloading zone caused by the stress-induced anisotropy

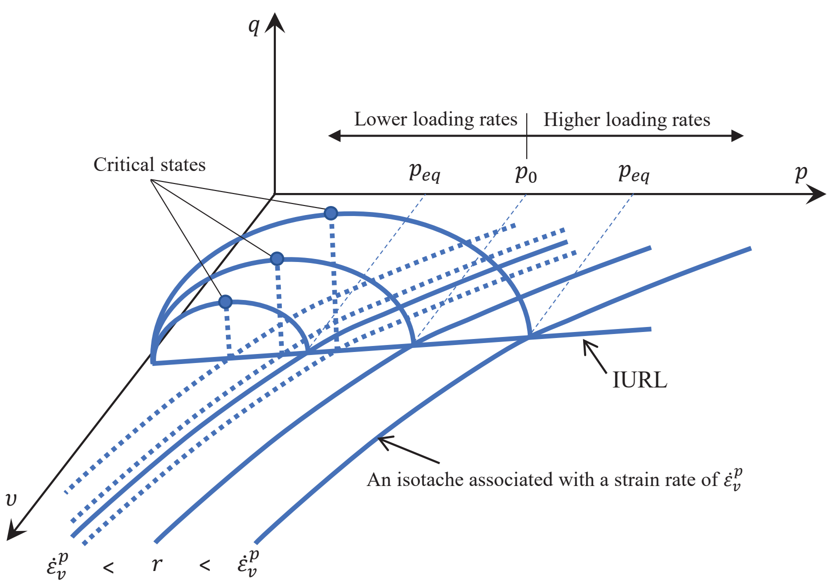

Fig. 5: Schematic illustration of the basic viscoplastic model with the homothetic MCC surfaces

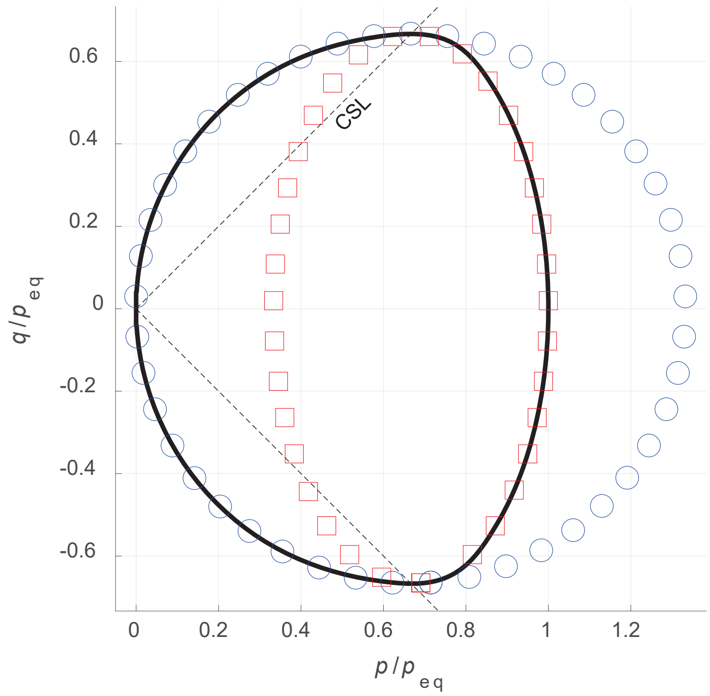

(a)

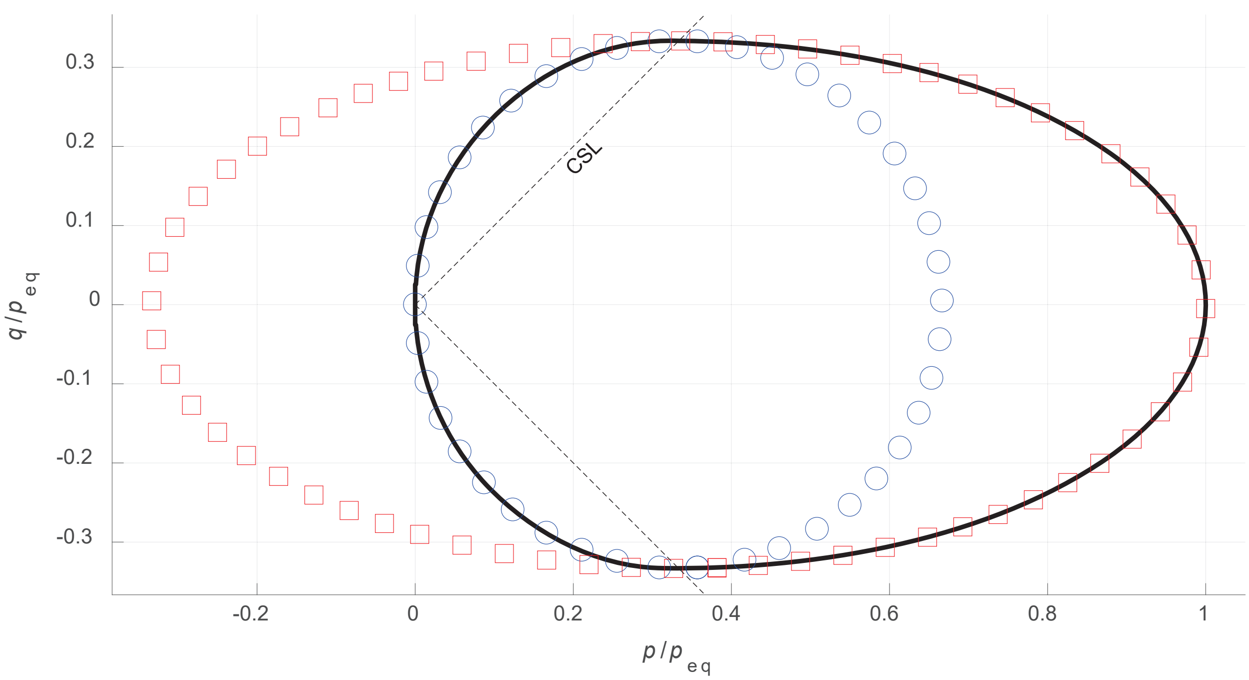

(b)

Fig. 6: The convex set in the true stress space when M = 1 and: (a) R = 1.5 (b) R = 3.0

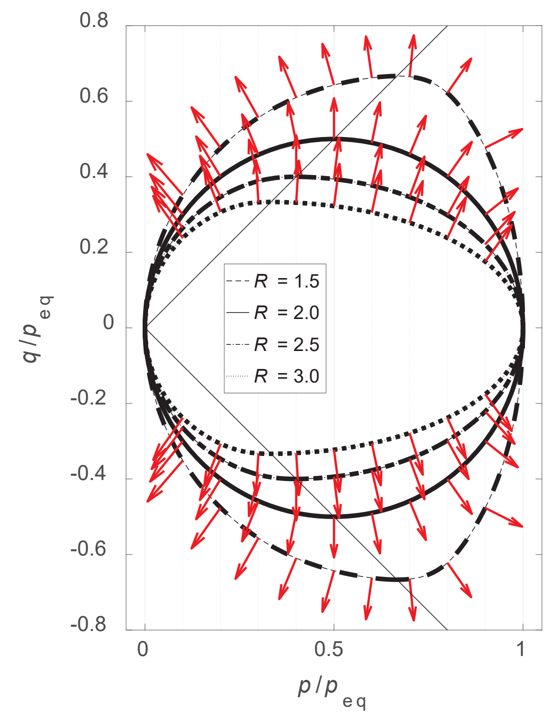

Fig. 7: The convex loci together with the corresponding inelastic flow directions (arrows) in the normalized true stress space for different values of R while M = 1

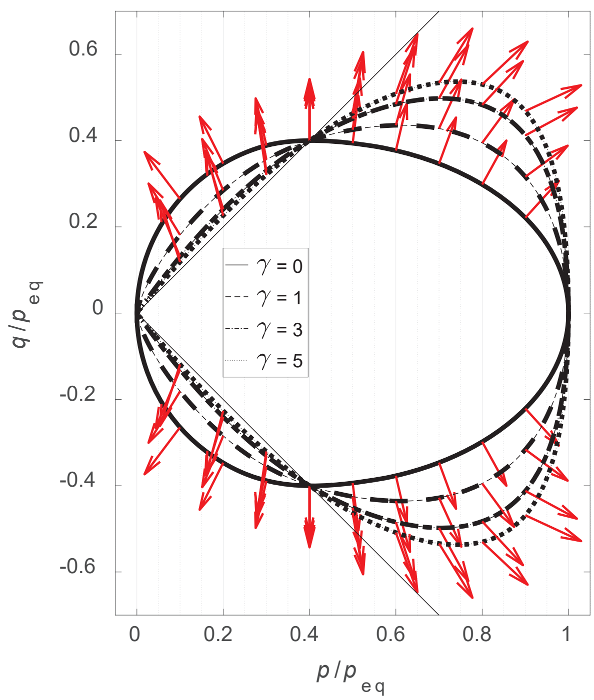

Fig. 8: The convex loci together with the corresponding inelastic flow directions (arrows) in the normalized true stress space for different values of γ while $\mathrm{M} = 1$ and $\mathrm{R} = 2.5$

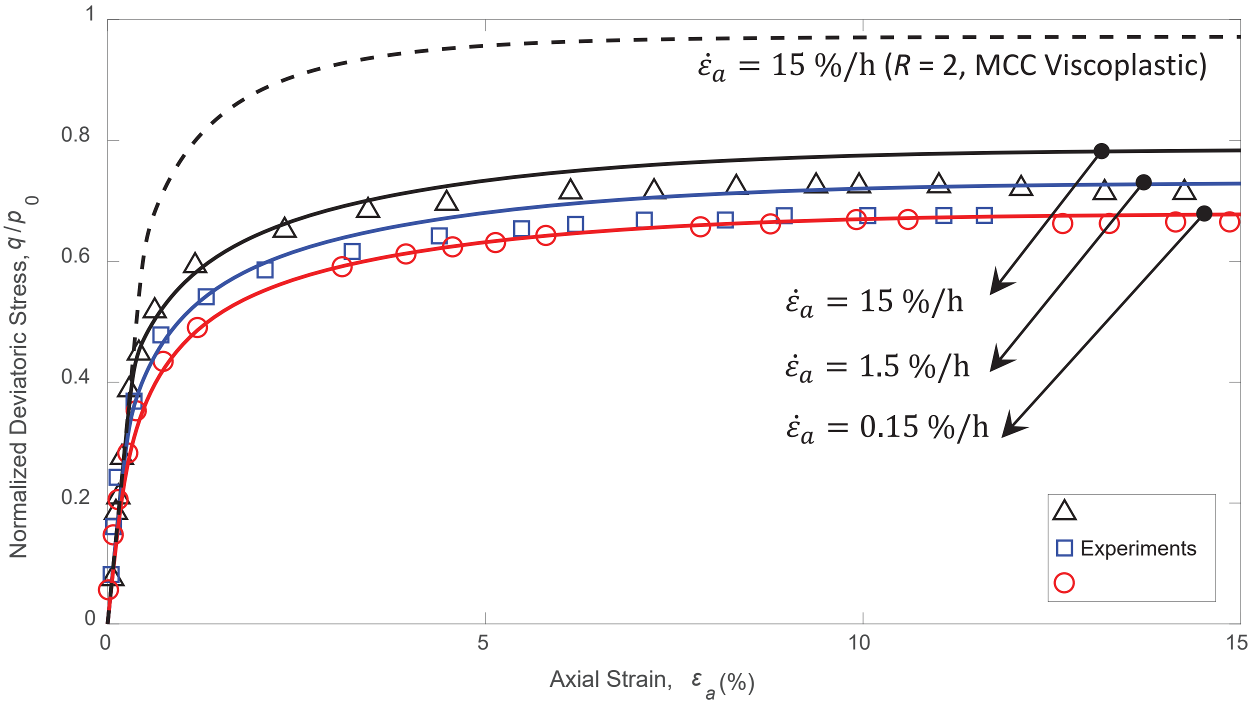

(a)

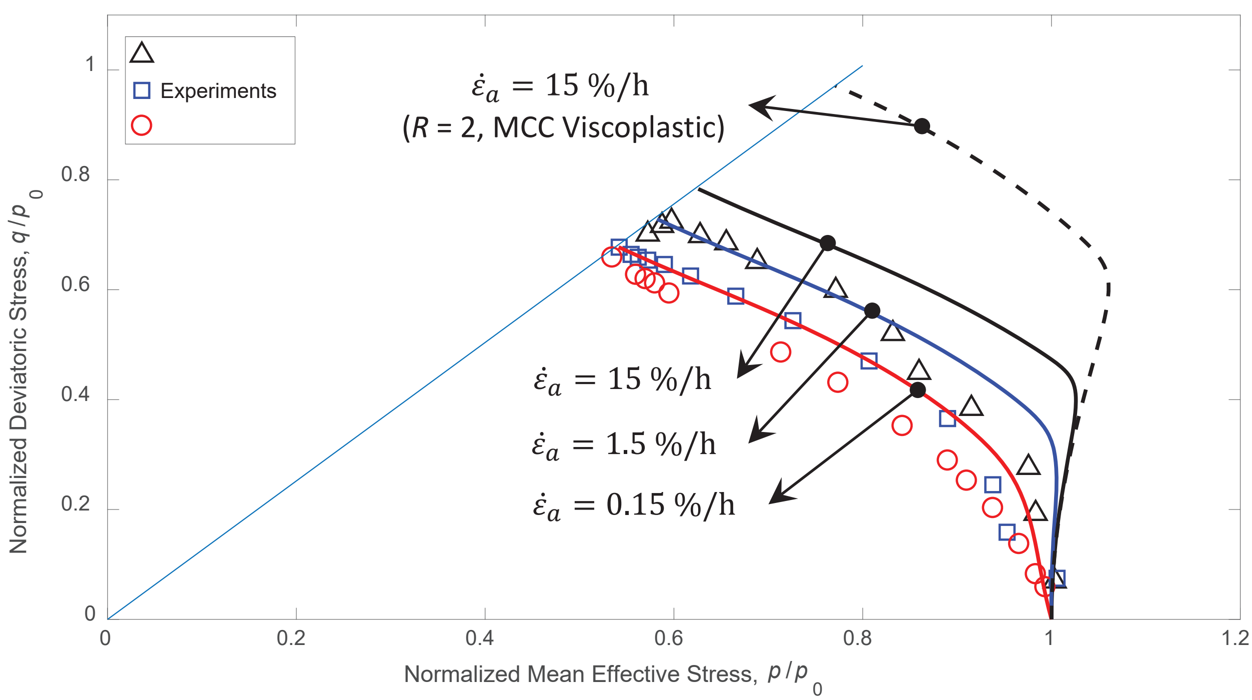

(b)

Fig. 9: Experimental and simulated undrained triaxial compression tests on normally consolidated reconstituted HKMD under different strain rates

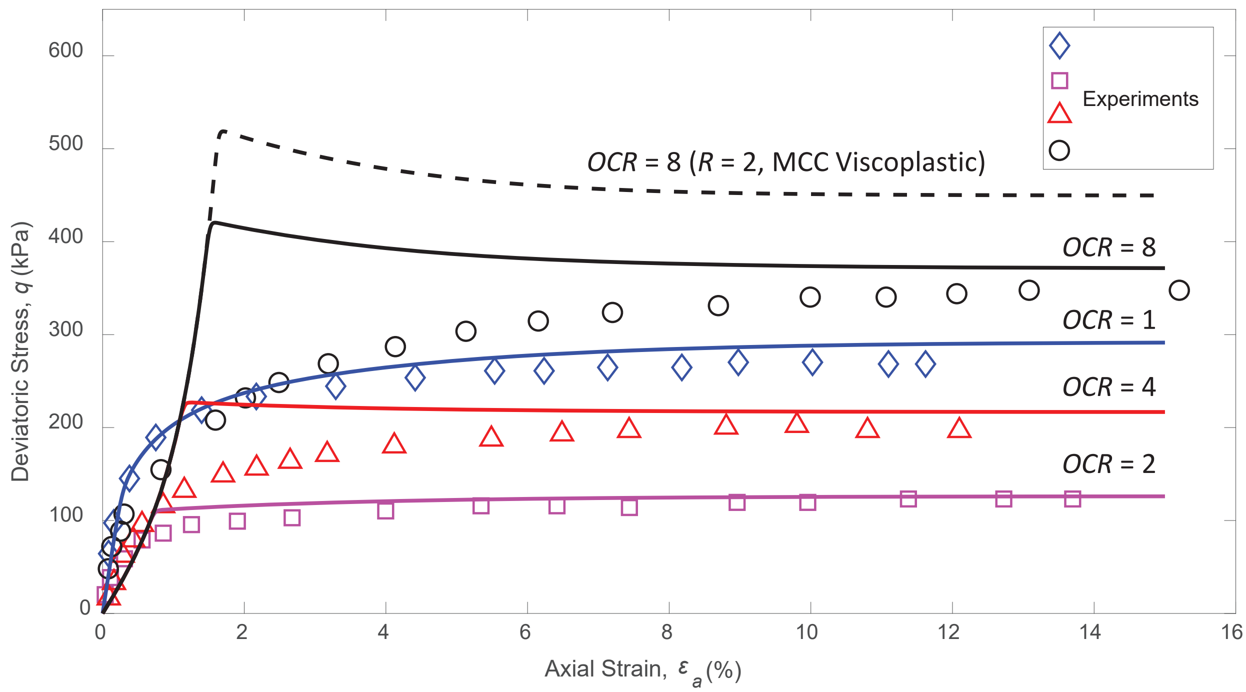

(a)

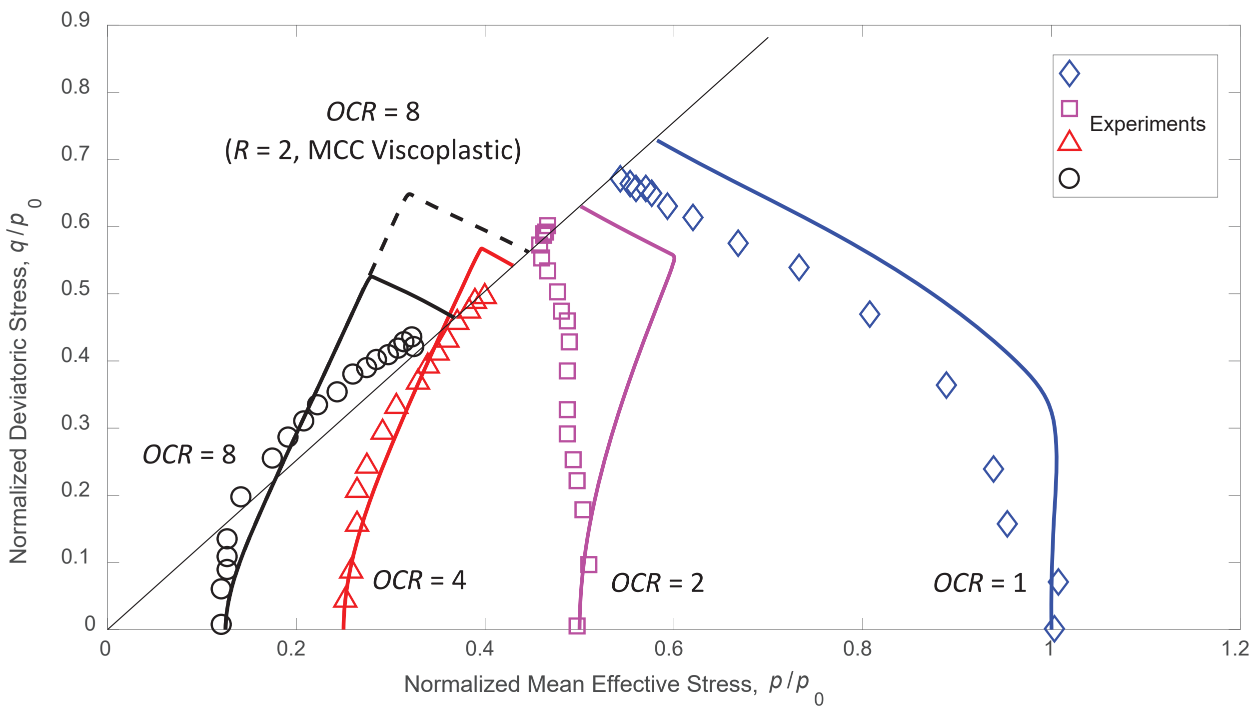

(b)

Fig. 10: Experimental and simulated undrained triaxial compression tests on reconstituted HKMD with different OCRs under constant axial strain rate of 1.5%/h

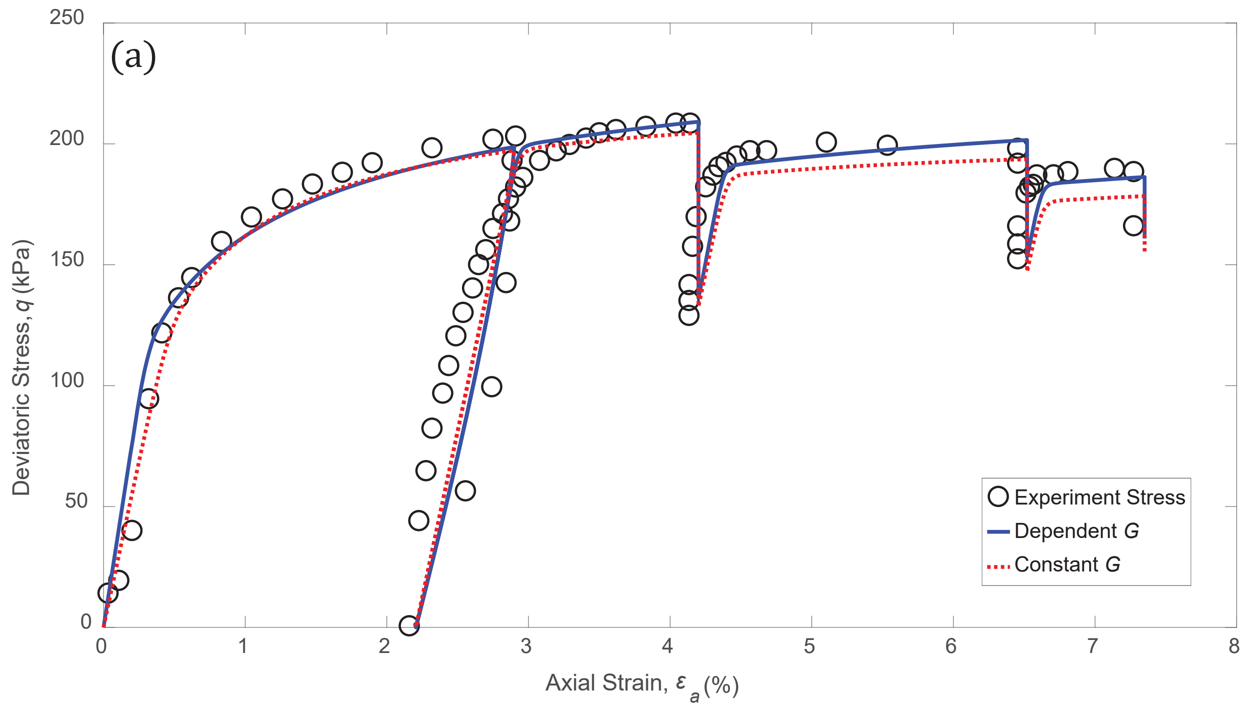
(a)
Deviatoric Stress, q (kPa)
Axial Strain, εa (%)
Experiment Stress
Dependent G
Constant G
0
50
100
150
200
250
0
1
2
3
4
5
6
7
8

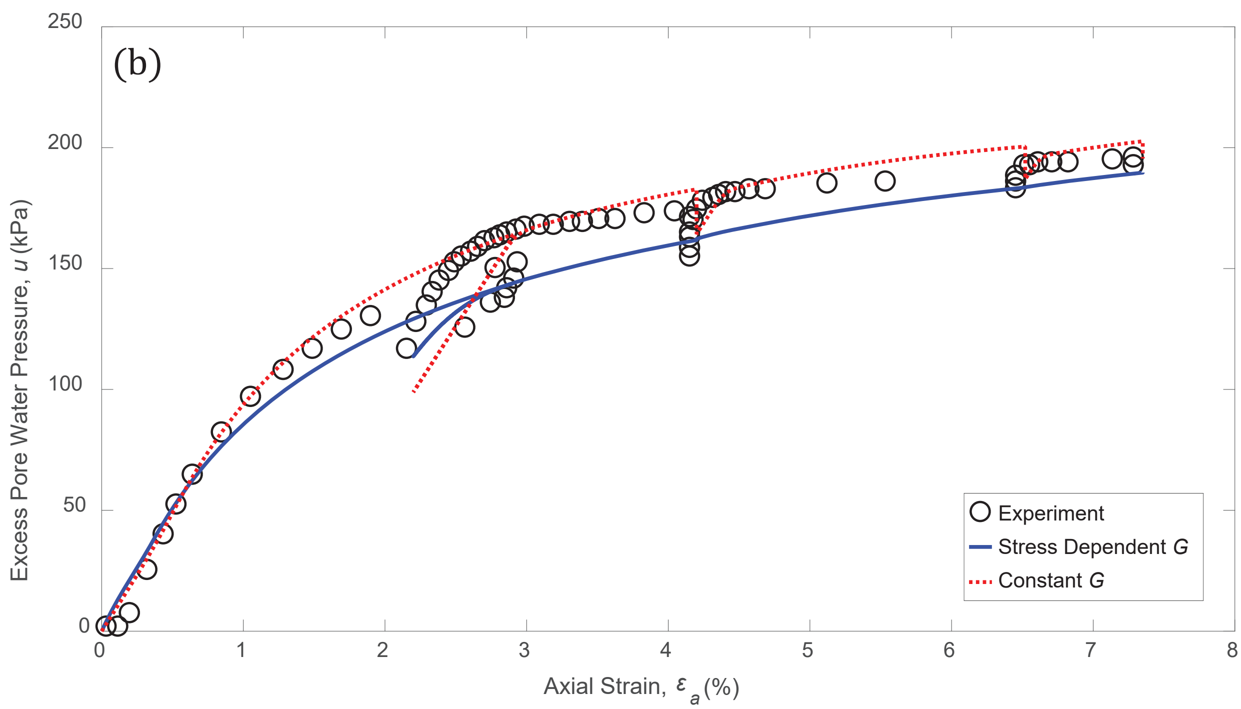
(b)
Excess Pore Water Pressure, u (kPa)
Axial Strain, εa (%)
Experiment
Stress Dependent G
Constant G
0
50
100
150
200
250
0
1
2
3
4
5
6
7
8

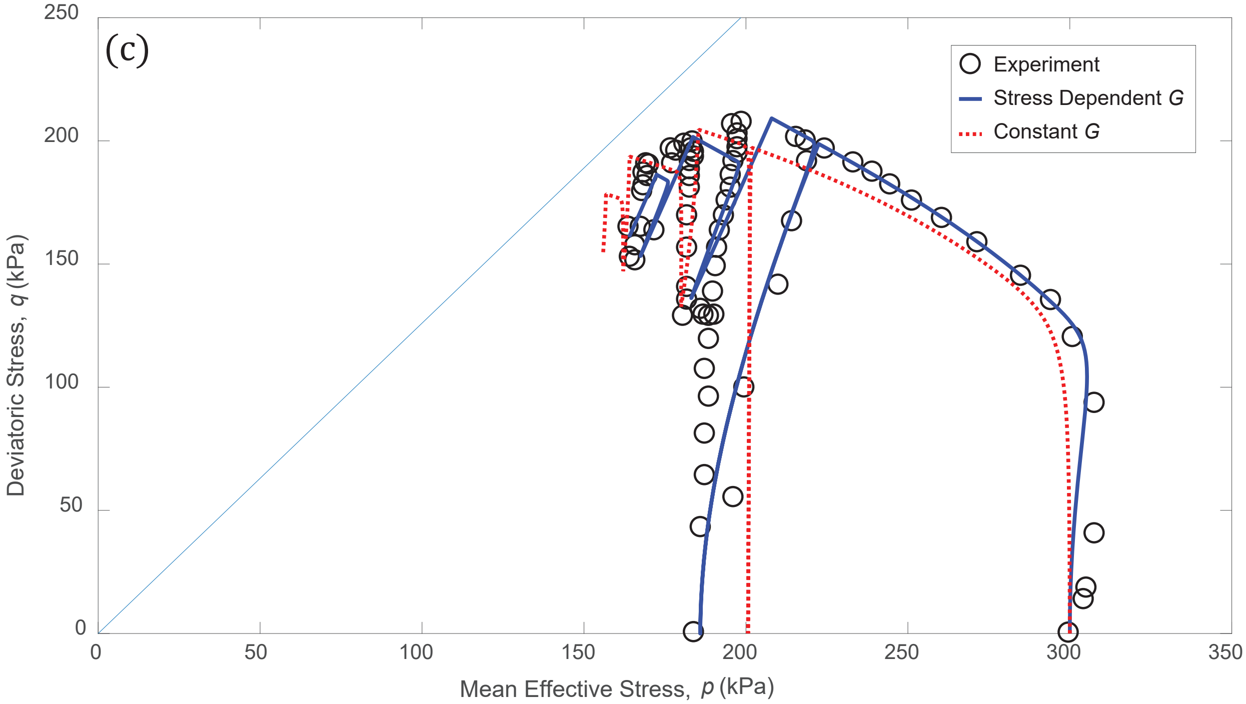

Fig. 11: Experimental and simulated results of multi-stage undrained triaxial compression test on reconstituted and normally consolidated HKMD in terms of (a) deviatoric stress vs axial strain; (b) excess pore water pressure vs axial strain; (c) deviatoric stress vs mean effective stress

Table 1: Parameters of the model and their values for HKMD

Model parameters	**Description**	**Value**
κ	the slope of the isotropic unloading-reloading line (IURL) in the logarithmic compression plane	0.018
λ	the slope of normal compression line (NCL) in the bi-logarithmic compression plane	0.0793
g	Dimensionless shear modulus coefficient	42
M	The slope of the critical state line in the p-q stress plane	1.26
R	Spacing ratio	2.5
γ	parameter for non-associated flow rule due to the frictional dissipation	0
μ	Creep index	0.0025

Table 2: Loading history of the multi-stage triaxial compression test on HKMD

Schedule	Loading	Unloading	Reloading	Relaxation	Loading	Relaxation	Loading	Relaxation
Axial strain rate (1/min)	0.1%	-0.1%	0.1%	0	0.01%	0	0.001%	0
Duration (min)	29	7	20	2540	232	1320	830	705